

High Transparency Iron Doped Indium Oxide ($\text{In}_{2-x}\text{Fe}_x\text{O}_3$, $x = 0.0, 0.05, 0.25, 0.35$ and 0.45) Films Prepared by the Sol-gel Method

(Filem Indium Oksida Terdop Ferum ($\text{In}_{2-x}\text{Fe}_x\text{O}_3$, $x = 0.0, 0.05, 0.25, 0.35$ dan 0.45)

Berlutsinar Tinggi yang Disediakan dengan Kaedah Sol Gel)

N.B. IBRAHIM*, H. BAQIAH & M.H. ABDULLAH

ABSTRACT

High quality indium oxide and iron doped indium oxide nanocrystalline films were prepared by the sol-gel method followed by a spin coating technique. The samples were characterized by an X-ray diffractometer, an atomic force microscopy and a UV-vis spectroscopy. All samples had good crystallinity with a preferred orientation in the (222) direction. The crystallite size increased from 12.1 nm for the pure sample to 16.1 nm for the sample with $x=0.35$ and then decreased to 12.1 nm for the sample with $x=0.45$. All samples contained nanometer grain sizes with a smooth surface. All films showed a high transmission of over 91% in the wavelength range of 200-800 nm.

Keywords: Crystallization; indium oxide; transmission

ABSTRAK

Filem nanohablur indium oksida dan indium oksida terdop ferum berkualiti tinggi telah disediakan dengan kaedah sol-gel diikuti dengan teknik salutan berputar. Sampel dicirikan dengan meter pembelauan sinar-X, mikroskop daya atom dan spektroskopi sinar nampak – UV. Kesemua sampel mempunyai penghabluran yang baik dengan orientasi pada arah (222). Saiz hablur meningkat daripada 12 nm untuk sampel tulen ke 16.1 nm untuk sampel $x=0.35$ dan berkurangan kepada 12.1 untuk sampel $x=0.45$. Kesemua sampel mengandungi butiran bersaiz nanometer dan permukaan yang rata. Kesemua sampel menunjukkan transmisi yang tinggi melebihi 91% dalam julat panjang gelombang 200 - 800 nm.

Kata kunci: Indium oksida; penghabluran; transmisi

INTRODUCTION

Transparent semiconductor oxides (TCO) become an important topic in materials science research because they have high transparency and good electrical conductivity thus can be used in many applications such as in flat panel displays, solar cells and gas sensors. Recently there are many papers reporting on the magnetic properties of these materials after being doped by a small amount of transition metal (Gao et al. 2010; Gupta et al. 2007; Li et al. 2007; Reddy et al. 2007; Sharma et al. 2003; Yoo et al. 2005; Zhao et al. 2009). The possibility of using TCO in a spintronic device may result in real size spintronic and opto-electronic devices (Kim et al. 2007; Munawar et al. 2011; Pearton et al. 2003).

Indium (III) oxide (In_2O_3) is a transparent conductor oxide (TCO) with a wide band gap, i.e 3.6 eV. Doping In_2O_3 with other elements could improve its physical properties. It has been reported that doping In_2O_3 with tin improves its electrical property thus making it suitable for application such as an electrode in solar cells, photovoltaics and flat panel displays (Antonia 2011; Kang et al. 2011; Li et al. 2010; Manavizadeh et al. 2009) while doping with Ba was reported to induce its sensing property to NO_x gas (Shekhar et al. 2011). Ferromagnetic properties can be induced in a

TCO by doping it with transition metals such as Fe, Ni, Cr and Mn (Gao et al. 2010; Gupta et al. 2007; Li et al. 2007; Reddy et al. 2007; Sharma et al. 2003; Zhao et al. 2009).

Iron is an attractive dopant for induction of magnetic properties in indium oxide because of its high solubility in the matrix. Iron doped indium oxide film has been prepared by laser ablation deposition and the sol-gel method (Gao et al. 2010; Yoo et al. 2005). The sol-gel method is a simple and low cost method. It also offers a precise control of the material composition (Chen et al. 2009; Shaiboub et al. 2012). Murakawa et al. (2004) proposed that iron doped indium thin film can be used as a high performance flat-panel display materials. In this paper iron doped indium oxide was prepared by the sol-gel method followed by a spin coating technique using indium nitrate hydrate, iron chloride hexahydrate and ethanol as a source, dopant material and reaction medium, respectively. The solvent used in the present work is different from the solvent used by Gao et al. (2010). The aims of this study were to study the effect of the iron dopant on the microstructure and optical properties of In_2O_3 films and to study the effect of different iron dopant values (x) on the microstructure and optical properties of $\text{In}_{2-x}\text{Fe}_x\text{O}_3$ films.

EXPERIMENTAL DETAILS

$\text{In}_{2-x}\text{Fe}_x\text{O}_3$ thin films were prepared by the sol-gel method followed by a spin coating technique. Indium nitrate hydrate ($\text{In}(\text{NO}_3)_3 \cdot \text{H}_2\text{O}$) and iron chloride hexahydrate ($\text{FeCl}_3 \cdot 6\text{H}_2\text{O}$) were used as the starting materials. Ethanol and acetylacetone were used as the solvents. Indium nitrate was first dissolved in a mixture of ethanol and acetylacetone while iron chloride was dissolved in ethanol. Each solution was stirred for 1 h at room temperature (30°C). The solutions were mixed and stirred for 2 h, then it was filtered using a $0.45 \mu\text{m}$ syringe filter and aged for 2 days. The aged solution was dropped onto a clean glass substrate and spin-coated at 1500 rpm for 30 s. The coated layer was dried at 70°C for 20 min to evaporate the organic solvent, followed by an annealing process at 500°C for 30 min to crystallize the films. The phase and crystal structure were investigated using a Bruker X-ray diffractometer (XRD) (2θ from 15 to 60°). The crystallite size of all samples was calculated using Scherrer's equation (Cullity 1978) as follows:

$$t = \frac{0.9\lambda}{B \cos\theta_E},$$

where t , λ , B and θ_B are the crystalline size, the wavelength of $\text{Cu K}\alpha$ ($\lambda=1.5406 \text{ \AA}$), width at half maximum (FWHM) in radian and Bragg angle, respectively. All parameters in the equations were determined from the analysis of XRD patterns using an EVA software. The surface morphology and roughness were studied using a Nova atomic force microscopy (AFM). The optical properties of the films were characterized using a Perkin Elmer (Lambda 35) UV-visible spectrophotometer.

RESULTS AND DISCUSSION

Figure 1 presents the X-ray diffraction patterns of undoped and Fe doped indium oxide thin films. All samples showed good match with pure In_2O_3 (JCPDS card number 006-0416). They are single phase polycrystallines with strong preferential orientation along (222) direction. Their structures are cubic with Ia-3 space group. There is no peak observed related to iron oxide or its compound. The peaks refer to doped samples clearly shift to a higher angle, indicating that the iron atoms have been incorporated into the In_2O_3 structure (Yoo et al. 2005). This shift are due to the replacement of indium atom, $R_{\text{In}^{3+}}=0.80 \text{ \AA}$ by a smaller ion size of iron, $R_{\text{Fe}^{3+}}=0.645 \text{ \AA}$ (Shannon 1976). This can also be confirmed from the lattice parameter calculation. The lattice parameter was calculated using full pattern matching function in the EVA software. In this function, the XRD pattern was fitted with the standard data (JCPDS 006-0416) using an empirical model for a peak shape. The lattice parameter of undoped sample ($x=0$) is 10.1052 \AA which is less than the standard value for bulk In_2O_3 (10.1180 \AA). The lattice parameters for all samples are summarized in Table 1. These results showed that the Fe solubility in these samples is similar as reported by Yoo et al. (2005). They reported the solubility of iron in indium oxide is 20%. These XRD results also showed that the annealing temperature of 500°C is sufficient to fully crystallize the samples.

Table 2 shows the XRD peaks intensities ratio between the XRD peak and the highest XRD peak. The results clearly show that the sample containing the highest dopant gives the highest intensities ratio meaning that it has the best crystallinity.

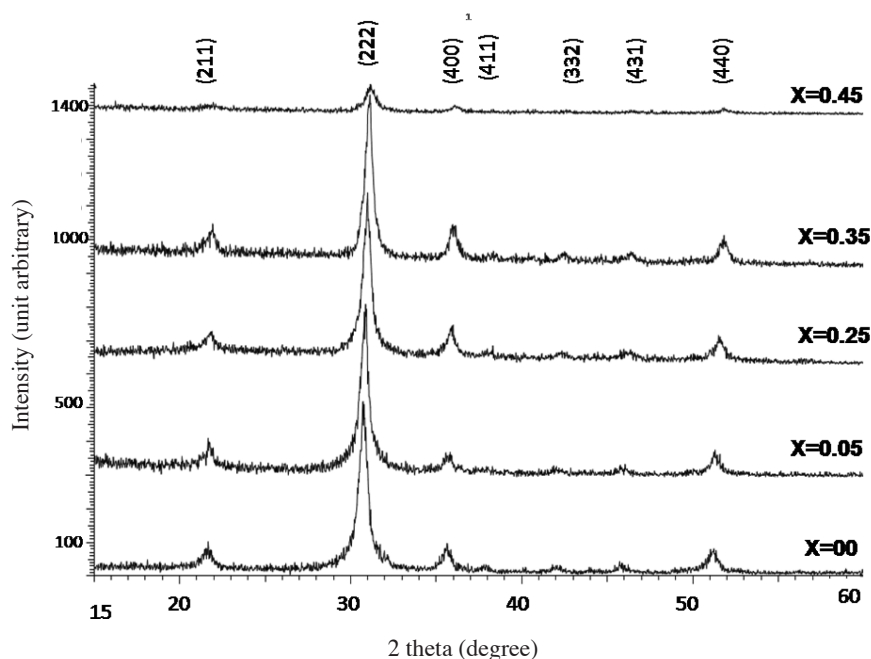


FIGURE 1. XRD pattern of $\text{In}_{2-x}\text{Fe}_x\text{O}_3$ thin film ($x=0, 0.05, 0.25, 0.35, 0.45$)

TABLE 1. The lattice parameter, relative reliability, crystal size, grain size, root mean square roughness, thickness and energy band gap of $(\text{In}_{1-x}\text{Fe}_x)_2\text{O}_3$ ($x=0.0, 0.05, 0.25, 0.35, 0.45$) thin films

Iron concentrations (x)	Lattice parameter (Å)	Relative reliability	Crystal size (nm)	Average grain size (nm)/ Standard deviation	Root Mean Square roughness (nm)	Thickness (± 0.1 nm)	Energy band gap (eV)
0	10.1052	1.3	12.1	19.5/8	2	92.3	3.76 \pm 0.06
0.05	10.0989	1.3	13.73	24/10	2	50.0	3.74 \pm 0.06
0.25	10.0238	1.04	14.3	35/9	1.2	62.0	3.73 \pm 0.07
0.35	10.0232	1.06	16.1	66/17	1.8	65.0	3.72 \pm 0.08
0.45	9.9781	1.28	12.1	15.5/5	0.96	77.6	3.78 \pm 0.08

TABLE 2. The peaks intensities ratio between the peak and the highest peak for all samples

x	I*	I ₁	I ₂	I ₃	I ₄	I ₅	I ₆	I ₇	I ₁ /I*	I ₂ /I*	I ₃ /I*	I ₄ /I*	I ₅ /I*	I ₆ /I*	I ₇ /I*
0	309	59	309	58	16	15	20	44	0.19	1	0.19	0.06	0.05	0.06	0.14
0.05	250	55	250	35	12	15	18	34	0.22	1	0.14	0.05	0.06	0.07	0.14
0.25	414	83	414	94	36	29	30	70	0.20	1	0.23	0.09	0.07	0.07	0.17
0.35	348	77	348	85	29	32	30	64	0.22	1	0.24	0.08	0.10	0.09	0.18
0.45	89	36	89	27	14		10	18	0.40	1	0.30	0.16		0.11	0.20

I*:highest intensity; I₁, I₂, I₃, I₄, I₅, I₆, I₇ : other peak intensities

The crystallite size of all samples was calculated from the most intense peak i.e. (222). The crystallite size of undoped sample is 12.1 nm. The increment of iron dopant ($x=0.05-0.35$) produces film with bigger crystallite size, however at $x=0.45$ the size decreases to 12.3 nm (Table 1). A similar result was reported by other researchers for Tb doped yttrium iron garnet films (Ftema et al. 2012) and Sn and Au thin films deposited on glass (Chopra 1969). The film thickness dominates the increment of lattice parameter (Chopra 1969).

Figure 2 shows the three dimensional AFM images of the samples. It can be seen that the grain sizes of indium oxide increase with the iron concentration up to $x=0.35$, however the grain sizes decrease at $x=0.45$. The size of the crystallite is smaller than the grain size because the grain consists of many crystallites. The measurement of surface roughness shows that all samples have smooth surfaces (Table 1).

The optical transmission of the samples is shown in Figure 3. All samples showed high transmission (over 91%) in the wavelength range of 200-800 nm. These values are higher than the results reported by Gao et al. (2010). They reported transmission of 75 - 85% for their 50 nm thickness Fe doped In_2O_3 films prepared using ethylene glycol monomethyl as a solvent. Even though their films were also prepared using the sol-gel method, the solvent used to dilute the precursor is different. It has been reported that the microstructure of a sol-gel thin film can be changed by using a different type of solvent (Hong et al. 2008). Since a film microstructure is related to the optical properties of

the films, changing the solvent could produce a film with different optical properties.

Figure 3 also shows that the transmission curves of doped samples have a small red shift as iron concentration increases, however sample $x=0.45$ has a small blue shift. This shifting indicates the change of the energy band gap of indium oxide due to iron doping.

The absorption coefficient of films can be calculated from the film transmission spectra using Lambert's law:

$$I = I_0 \exp(-\alpha t),$$

where I_0 is the incident light intensity, I is the transmitted light intensity, α is the absorption coefficient and t is the film thickness. Then the α can be used to calculate the optical energy gap using Tauc's equation:

$$(\alpha h\nu)^n = (h\nu - E_g),$$

where α is the absorption coefficient of the film, $h\nu$ is the photon energy and E_g is the energy gap, n is a constant which depends on the transition process: $n=2$ for allowed direct transition, $2/3$ for forbidden indirect transition, $1/2$ for allowed indirect transition and $1/3$ for forbidden indirect transition. The band gap was estimated from the relation between $(\alpha h\nu)^2$ vs $h\nu$. This relation is a parabolic curve and the energy gap was estimated by extrapolation a straight line from the linear part to intersect at $h\nu$ axis, giving the E_g value. In our calculation, n is fixed to 2 because the extrapolation line has maximum regression value at $n=2$.

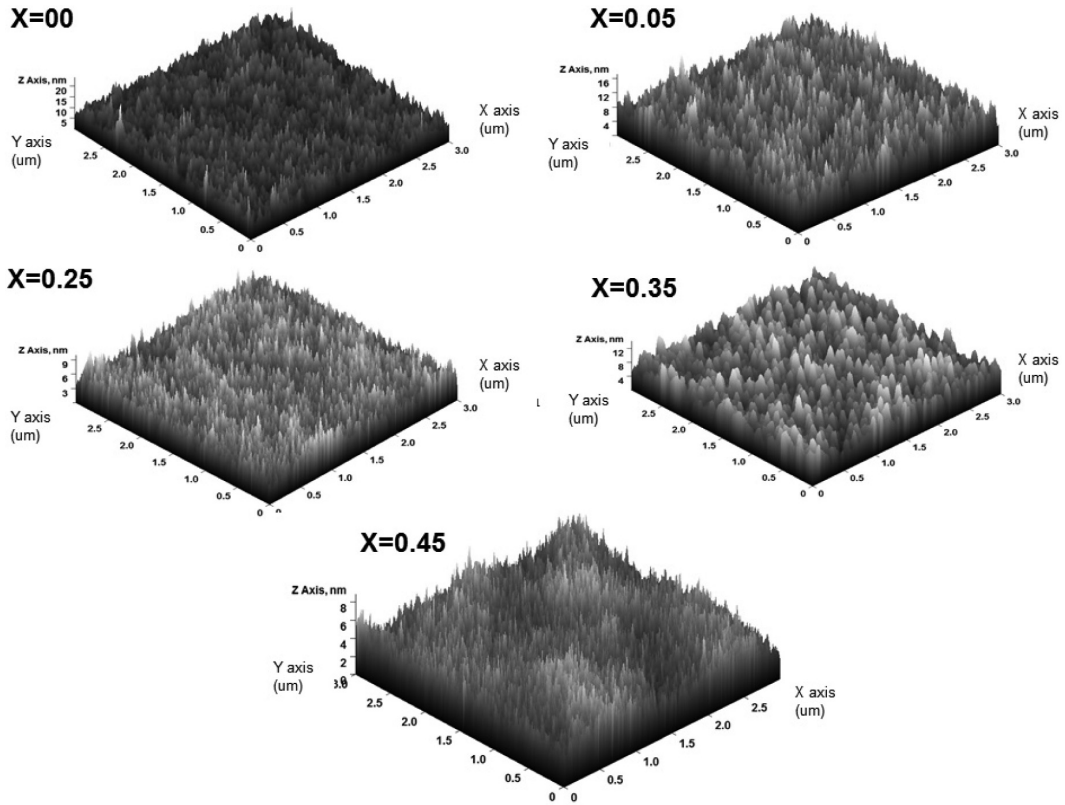


FIGURE 2. AFM micrograph of $In_{2-x}Fe_xO_3$ ($x=0.0, 0.05, 0.25, 0.35, 0.45$)

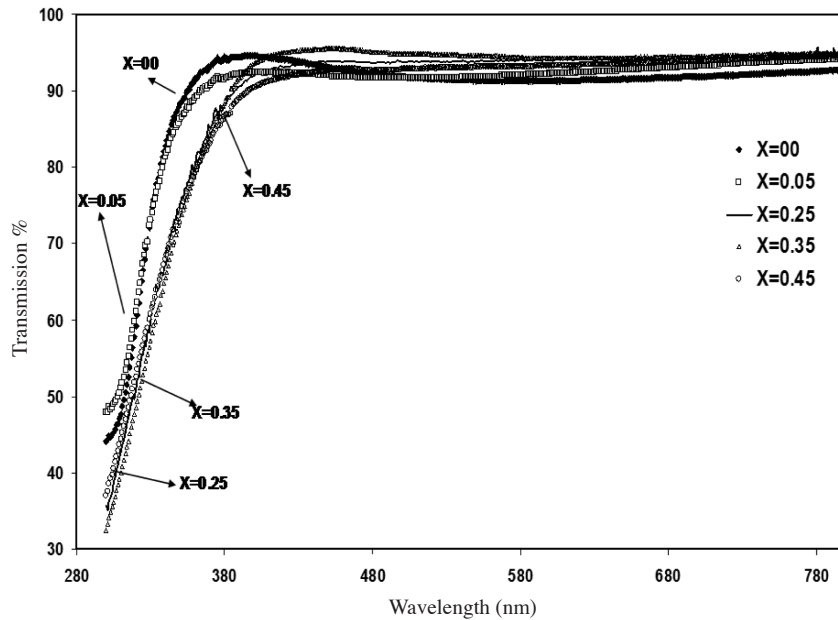


FIGURE 3. Optical transmission spectra of $In_{2-x}Fe_xO_3$ thin film ($x=0.0, 0.05, 0.25, 0.35, 0.45$)

Figure 4 shows the optical absorption coefficient vs wavelength for all samples. Iron dopant effects the coefficient but in a non systematic way.

The band gap for pure sample is 3.76 eV which is higher than bulk In_2O_3 (3.6 eV) due to the smaller grain sizes. This result is similar to the result reported by Kong et al. (2011)

for their (222) oriented indium oxide thin film deposited on MgO (100) substrate. The band gap decreases as the iron concentration increases up 3.72 eV for sample with $x=0.35$. Similar result has also been reported elsewhere for Mn doped indium tin oxide (ITO) thin film prepared by sol-gel method (Reddy et al. 2007). The E_g decreases from 3.77 to 3.72 eV

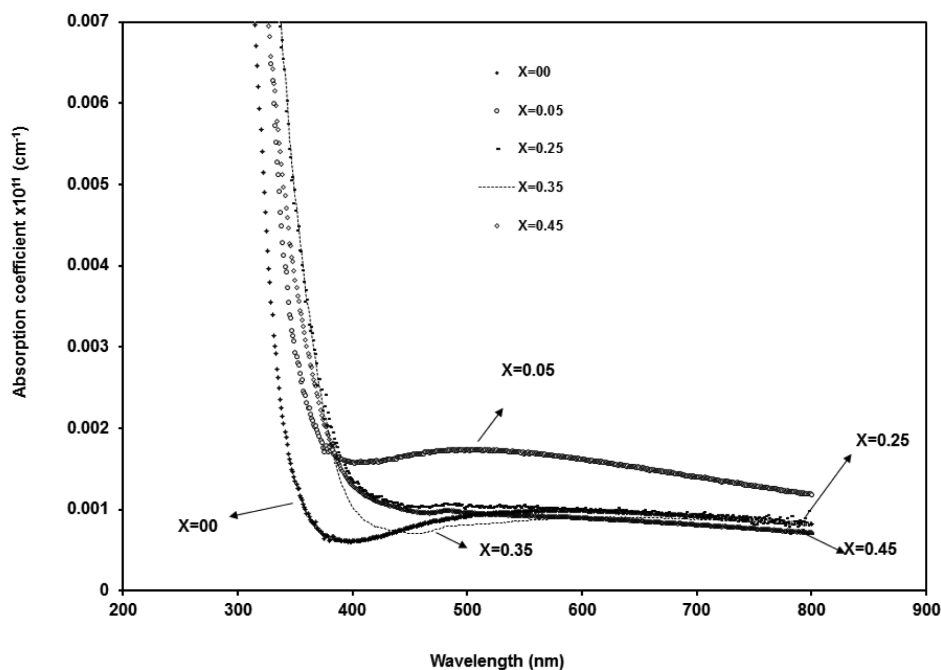


FIGURE 4. Absorption coefficient vs wavelength for $\text{In}_{2-x}\text{Fe}_x\text{O}_3$ thin film ($x=0.00, 0.05, 0.25, 0.35, 0.45$)

as the Mn concentration increases from 3% to 4%. This result could be associated with the reduce of electron energies due to the many body effect of free carriers caused by highly doping concentration in semiconductors (Schubert 2007). However, the band gap increases to 3.78 eV for sample $x=0.45$. The modification of energy gap of chromium doped indium oxide prepared on (001) Si and yttria-stabilized zirconia (YSZ) was reported to be caused by the crystal structural transition (Hsu 2012). Hsu (2012) reported that the optical band gap of their chromium doped indium oxide showed a maximum at the intermediate state and decreased, respectively, towards high and less ideally crystallized states. In the present study, it is believed that the increment of the band gap in sample $x=0.45$ could be related to the changes in the microstructure of indium oxide as shown from the XRD results.

CONCLUSION

The iron solubility in the In_2O_3 thin film prepared by the sol-gel method followed by the spin coating technique was as high as reported by other researches i.e. ~20%. $\text{In}_{2-x}\text{Fe}_x\text{O}_3$ ($x=0.0, 0.05, 0.25, 0.35$ and 0.45) film were successfully prepared without any impurities. The crystallite sizes increase from 12.1 for pure sample to 16.1 nm for $x=0.35$. The grain sizes calculated from AFM scan analysis showed that all samples contain nanometer grains sizes. All samples have smooth surface and high transmission i.e. over 91% which were higher than being reported by previous researchers for iron doped In_2O_3 . Iron dopant effect the optical absorption of the samples. The calculated band gaps decreased from 3.76 eV for pure to 3.72 eV for sample $x=0.35$.

ACKNOWLEDGEMENT

This work was supported by the Malaysian Ministry of Science, Technology and Innovation via grant No. 03-01-02-SF0742 and Universiti Kebangsaan Malaysia (UKM-OUP -FST -2012).

REFERENCES

- Antonia Sonia Alves Cardoso, D. 2011. The effects of various annealing regimes on the microstructure and physical properties of ITO ($\text{In}_2\text{O}_3:\text{Sn}$) thin films deposited by electron beam evaporation for solar energy applications. *Renewable Energy* 36(4): 1153-1165.
- Chen, H.Z., Kao, M.C., Young, S.L., Yu, C.C., Lin, C.H., Lee, C.M. & Ou, C.R. 2009. Effects of annealing atmosphere on microstructure and ferroelectric properties of praseodymium-doped $\text{Bi}_4\text{Ti}_3\text{O}_{12}$ thin films prepared by sol-gel method. *Thin Solid Films* 517(17): 4818-4821.
- Chopra, K.L. 1969. *Thin Film Phenomena*. New York: McGraw-Hill, Inc.
- Cullity, B.D. 1978. *Elements of X-ray Diffraction*. 2nd ed. New York: Addison-Wesley Pub. Co. Inc. p. 102.
- Ftema, W., Aldbea, Ibrahim, N.B., Mustafa Hj Abdulah & Ramadan, E.S. 2012. Structural and magnetic properties of $\text{TbxY}_{3-x}\text{Fe}_5\text{O}_{12}$ ($0 \leq x \leq 0.8$) thin film prepared via sol-gel method. *Journal of Sol-gel Science and Technology* 62(3): 483-489.
- Gao, H., Zhigang Sun, Wei Duan, Yanbing Chen & Mi Li. 2010. Magnetism regulation of $(\text{In}_{1-x}\text{Fe}_x)_2\text{O}_3$ semiconductors prepared by sol-gel method. *Journal of Wuhan University of Technology--Materials Science* 25(1): 20-23.
- Gupta, A., Hongtao Cao, Kinnari Parekh, Rao, K.V., Raju, A.R. & Waghmare, U.V. 2007. Room temperature ferromagnetism in transition metal (V, Cr, Ti) doped In_2O_3 . *Journal of Applied Physics* 101(9): 09N513-513.

- Hong Li, Gaoling Zhao, Bin Song & Gaorong Han. 2008. Preparation of macroporous and mesoporous TiO₂ film with various solvent. *Materials Letters* 62: 3395-3397.
- Hsu, C.Y. 2012. Effects of crystalline structural transition on electronic-band structure of chromium-doped indium oxide. *Thin Solid Films* 520(6): 2311-2315.
- Kang, D-W., Kuk, Seung-Hee., Ji, Kwang-Sun., Lee, Heon-Min & Han, Min-Koo. 2011. Effects of ITO precursor thickness on transparent conductive Al doped ZnO film for solar cell applications. *Solar Energy Materials and Solar Cells* 95(1): 138-141.
- Kim, K-C., Kim, Eung-kwon & Kim, Young-Sung. 2007. Growth and physical properties of sol-gel derived Co doped ZnO thin film. *Superlattices and Microstructures* 42(1-6): 246-250.
- Kong, L., Ma, J., Caina Luan, Zhen Zhu & Qiaoqun Yu. 2011. Domain structure and optical property of epitaxial indium oxide film deposited on MgO(100) substrate. *Surface Science* 605(9-10): 977-981.
- Li, X., Xia, C., Guangqing Pei & Xiaoli He. 2007. Synthesis and characterization of room-temperature ferromagnetism in Fe- and Ni-co-doped In₂O₃. *Journal of Physics and Chemistry of Solids* 68(10): 1836-1840.
- Li, Z-H., Cho, E.S. & Sang Jik Kwon. 2010. Laser direct patterning of the T-shaped ITO electrode for high-efficiency alternative current plasma display panels. *Applied Surface Science* 257(3): 776-780.
- Manavizadeh, N., Boroumand, F.A., Ebrahim Asl-Soleimani, Farshid Raissi, Sheida Bagherzadeh, Alireza Khodayari & Mohammad Amin Rasouli. 2009. Influence of substrates on the structural and morphological properties of RF sputtered ITO thin films for photovoltaic application. *Thin Solid Films* 517(7): 2324-2327.
- Munawar Basha, S., Ramasubramanian, S., Rajagopalan, M., Kumar, J., Tae Won Kang, Ganapathi Subramaniam, N. & Younghae Kwon. 2011. Investigations on cobalt doped GaN for spintronic applications. *Journal of Crystal Growth* 318(1): 432-435.
- Murakawa, Y.Y.K., Tajiri, T., Suzuka, T., Sasaki, M., Shimooka, H., Oku, M., Shishido, T. & Matsushima, S. 2004. Fe doping effects on the optical and magnetic properties of indium oxide. *Trans. Mater. Res. Soc. Jpn.* 29(4): 1509-1511.
- Pearson, S.J., Abernathy, C.R., Norton, D.P., Hebard, A.F., Park, Y.D., Boatner, L.A. & Budai, J.D. 2003. Advances in wide bandgap materials for semiconductor spintronics. *Materials Science and Engineering: R: Reports* 40(4): 137-168.
- Reddy, K., Hays, J., Kundu, S., Dua, L., Biswas, P., Wang, C., Shutthanandan, V., Engelhard, M., Mathew, X. & Punnoose, A. 2007. Effect of Mn doping on the structural, morphological, optical and magnetic properties of indium tin oxide films. *Journal of Materials Science: Materials in Electronics* 18(12): 1197-1201.
- Schubert, E.F. 2007. *Physical Foundations of Solid-State Devices*. New York: Rensselaer Polytechnic Troy Institute. p. 182.
- Shaiboub, R., Ibrahim, N.B. & Abdullah, M.H. 2012. The physical properties of erbium-doped yttrium iron garnet films prepared by sol-gel method. *Journal of Nanomaterials* 2012: 1-5.
- Shannon, R. 1976. Revised effective ionic radii and systematic studies of interatomic distances in halides and chalcogenides. *Acta Crystallographica Section A* 32(5): 751-767.
- Sharma, P., Gupta, A., Rao, K.V., Owens, F.J., Renu Sharma, Rajeev Ahuja, Osorio Guillen, J.M., Borje Johansson & Gehring, G.A. 2003. Ferromagnetism above room temperature in bulk and transparent thin films of Mn-doped ZnO. *Nature Material* 2(10): 673-677.
- Shekhar, C., Gnanasekar, K.I., Prabhu, E., Jayaraman, V. & Gnanasekaran, T. 2011. In₂O₃+ xBaO (x=0.5-5 at.%) - A novel material for trace level detection of NO_x in the ambient. *Sensors and Actuators B: Chemical* 155(1): 19-27.
- Yoo, Y.K., Xue, Q., Lee, H.C., Cheng, S., Xiang, X.D., Dionne, G.F., Xu, S., He, J., Chu, Y.S., Preite, S.D., Lofland, S.E. & Takeuchi, I. 2005. Bulk synthesis and high-temperature ferromagnetism of (In_{1-x}Fe_x)₂O₃-σ with Cu co-doping. *Applied Physics Letters* 86(4): 042506-042506-042503.
- Zhao, B.C., Xia, B., Ho, H.W., Fan, Z.C. & Wang, L. 2009. Anomalous hall effect in Cu and Fe codoped In₂O₃ and ITO thin films. *Physica B: Condensed Matter* 404(16): 2117-2121.

School of Applied Physics
Faculty of Science and Technology
Universiti Kebangsaan Malaysia
43600 Bangi, Selangor, D.E.
Malaysia

*Corresponding author; email: baayah@ukm.my

Received: 14 May 2012

Accepted: 27 November 2012